

# Engineering of Hyperentangled Complex Quantum Networks

Murad Ahmad,<sup>1</sup> Liaqat Ali,<sup>1,2,\*</sup> Muhammad Imran,<sup>3</sup> Rameez-ul Islam,<sup>3</sup>  
Manzoor Ikram,<sup>3</sup> Rafi Ud Din,<sup>4</sup> Ashfaq Ahmad,<sup>5</sup> and Iftikhar Ahmad<sup>1,6</sup>

<sup>1</sup>*Department of Physics, University of Malakand Chakdara, Dir Lower, KP, Pakistan*

<sup>2</sup>*Department of Physics, Government Degree College Lund Khwar Mardan, KP, Pakistan*

<sup>3</sup>*National Institute of Lasers and Optronics College Pakistan Institute  
of Engineering and Applied Sciences, Nilore, Islamabad, Pakistan*

<sup>4</sup>*Department of Physics, COMSATS University Islamabad, Islamabad, Pakistan*

<sup>5</sup>*Department of Chemistry, College of Science,  
King Saud University, P.O. Box, 2455, Riyadh-11451, Saudi Arabia*

<sup>6</sup>*Center for Computational Material Sciences,  
University of Malakand Chakdara, Dir Lower, KP, Pakistan*

Hyperentangled states are highly efficient and resource economical. This is because they enhance the quantum information encoding capabilities due to the correlated engagement of more than one degree of freedom of the same quantum entity while keeping the physical resources at their minimum. Therefore, initially the photonic hyperentangled states have been explored extensively but the generation and respective manipulation of the atomic counterpart states are still limited to only few proposals. In this work, we propose a new and feasible scheme to engineer the atomic hyperentangled cluster and ring graph states invoking cavity QED technique for applicative relevance to quantum biology and quantum communications utilizing the complex quantum networks. These states are engineered using both external quantized momenta states and energy levels of neutral atoms under off-resonant and resonant Atomic Bragg Diffraction (ABD) technique. The study of dynamical capacity and potential efficiency have certainly enhanced the range of usefulness of these states. In order to assess the operational behavior of such states when subjected to a realistic noise environment has also been simulated, demonstrating long enough sustainability of the proposed states. Moreover, experimental feasibility of the proposed scheme has also been elucidated under the prevailing cavity-QED research scenario.

**Keywords:** Hyperentangled states, Quantum Networks, Quantum Information, Quantum Optics

## I. Introduction

The development of fast, efficient and secure computational and communication techniques based on counterintuitive trait of quantum mechanics have led to the rapidly emerging field of quantum informatics [1–4]. In this regard, quantum state engineering measurement, large number of qubits scalability and long coherence times are the stringent prerequisite for the development of practical quantum technologies [5, 6]. Now, in the historical context, the entanglement has played a key role to address the foundational problems of quantum theory as well as to implement a multitude quantum information tasks [3, 7, 8]. It enables us to implement the efficient and successful quantum data transmission, processing and manipulation as well as to assess coherence retainment and losses in the quantum information encoded in a quantum system [9–11]. The rapid development of various entanglement-based quantum information protocols have ushered the subject matter to quite a mature stage by now [12, 13]. Moreover, for multi-party quantum communication, the quantum information needs to be distributed among many parties coherently bonded into a complicated entangled network morphology. Such quantum networks are naturally found in biological systems and may also potentially become the building block of quantum internet. These quantum networks have the capability to store the quantum information on their nodes which are interlinked through various quantum channels. In this way quantum information can be effectively and nonlocally distributed from one place to another making its dissemination quite practical throughout the whole network with high fidelity [14].

\* [liaqatphysicsuom@gmail.com](mailto:liaqatphysicsuom@gmail.com)

Now entanglement, a fundamental ingredient of quantum networks has been generated through various experimental techniques by utilizing the relevant specific degree of freedoms (DOF) associated with a physical system. Such a coherent quantum correlation is generally engineered using a single DOF of many parties i.e. photon's polarization frequency or the spatial modes, spin of electron, energy levels of an atom or its external momenta states. Whereas, entanglement of more than one degree of freedom is commonly referred to as the hyperentangled state for two or more parties [15]. Till now, the photonic systems have been extensively studied and are assumed to be the major resource of hyperentangled states generation. However, atomic systems have also been recently utilized for the hyperentangled states engineering and manipulation [16–19]. Such atomic hyperentangled states employ the quantized atomic internal and external DOFs. It is well known that the addition of an extra DOF in an entangled state will enhance the quantum communication channel capacity logarithmically i.e.  $2^n$  [20], and hence boost the quantum information tasks such as hyperentanglement purification [21], hyperentanglement teleportation [22–26], Bell state analysis [27] and hyperentanglement concentration [28] while keeping the physical resource level at its bare minimum. The atomic hyperentangled states are generally engineered through Atomic Bragg Diffraction (ABD) [17–19]. It is important to note that ABD, an experimentally feasible tool, has already been employed to handle several quantum foundational issues as well as the quantum state engineering and processing tasks [29–32].

In the present work, we proposed schematics to engineer a number of hyperentangled graph states with diverse morphologies such as  $n$ -partite linear quantized momenta cluster states, 2D cluster states and ring graph states through Atomic Bragg Diffraction technique. The cluster states especially 2D-cluster states serve as the fundamental resource for the measurement based one-way quantum computing model [33, 34]. This model encompasses such states as a computational resource and step by step processes the information through single-qubit measurements. In this regard, the experimental possibility of this model has already been tested in a significant way through the manipulation of 4-photon cluster state [35]. Moreover, these states can be utilized for any complex multi-gate quantum information protocol due to their strong natural decoherence resistance, stability and inherently deterministic nature [36]. Keeping in view the vitality and versatility of such states, a plethora of proposals regarding cluster state engineering in solid-state, atomic and photonic systems through diverse techniques have been put forward in the recent decades while hinting out their respective applicability for one-way computing [37–56]. On practical backgrounds, the linear optic techniques based schemes have already been demonstrated experimentally [35, 57, 58]. These techniques are, in general, probabilistic and become difficult to implement experimentally with the increase in the state dimensionality and the subsequent additive nature of net failure probability. However, the techniques based on cavity QED are inherently deterministic, the atomic states under realistic experimental conditions, can produce such graph states with probability of success approaching unity [33–35, 59–62]. Furthermore, spontaneous emission, a usual constraint on state coherence in atom-field cavity QED systems do not pose any significant threat on the dimensionality of the graph states being engineered, because here we are playing with the off-resonant ABD that involves only virtual Rabi cycles with no real absorption or emission process invoked.

The present work is arranged as follows: section-I is a brief introduction to the problem. Section-II is an overview of the mathematical tool i.e. ABD for the tagging of atoms with the cavities in momentum space leading to the subsequent state engineering. Section-III narrates in detail the engineering of various hyperentangled graph states. The last section provides a summary along with the discussion over the envisioned merits of the presented schematics. This section also elucidates briefly over the experimental feasibility of the proposed work in the context of realistic and contemporary research scenario.

## II. Tagging of atoms in momentum space

We consider the two different sets of two-level neutral atoms, one to engineer the hyperentangled states called type-1 atoms. These type-1 atoms, apart from the discrete energy levels, are also taken external quantized transverse momentum. The second type are auxiliary atoms used to erase the cavities quantum

information and are termed as type-2 atoms. They are considered quantized only in internal states and are used as the cavity information eraser through swapping via resonant interaction. The type-2 atoms are also employed for joining or entangling various independent quantum states through dispersive atom-field interactions much similar to the phase gate operation [63]. We also assume two high-Q cavities with both being taken initially to be in  $(|0_j\rangle + |1_j\rangle)/\sqrt{2}$  photon superposition states with  $j = 1, 2$ . Now the type-1 atoms, initially prepared in their ground states  $|b_j\rangle$  with momentum  $|P_{o_j}\rangle$ , interact off-resonantly with the cavities under Bragg regime cavity QED scenario as shown in Fig. 1. Thus the initial state vector for the first atom traversing the cavity-1 will be;

$$|\Psi(0)\rangle = \frac{1}{\sqrt{2}}[|0\rangle + |1\rangle] \otimes |b, P_o\rangle \quad (1)$$

Where  $|P_o\rangle = \hbar k$  is the quantized transverse atomic momentum along the cavity axis. The Hamiltonian for such an interaction under dipole and rotating wave approximation is [64];

$$H = \frac{\hat{P}_x^2}{2m} + \frac{\hbar\Delta}{2}\sigma_z + \hbar\mu\text{Cos}(kx)[\sigma_{ab}\hat{c} + \hat{c}^\dagger\sigma_{ba}] \quad (2)$$

Here  $\hat{P}_x^2/2m$  marks the kinetic energy along the axis of quantized atomic external momentum,  $\sigma_{ab} = |a\rangle\langle b|$ ,  $\sigma_{ba} = |b\rangle\langle a|$  and  $\sigma_z = |a\rangle\langle a| - |b\rangle\langle b|$  corresponds to the raising, lowering and inversion atomic operators. Whereas  $|b\rangle(|a\rangle)$  denotes the atomic ground (excited) state,  $\hat{c}(\hat{c}^\dagger)$  stands for the field annihilation (creation) operator and  $\Delta$  specifies the atom-field detuning while  $\mu$  is the Rabi frequency for such atom-field interaction. Now the proposed state vector for an arbitrary interaction time  $t$  will be [60, 64];

$$|\Psi(t)\rangle = \exp^{-i(\frac{P_x^2}{2m\hbar} - \frac{\Delta}{2})t} \sum_{l=-\infty}^{\infty} \left[ C_{(0,b)}^{(P_l)}(t)|0, b, P_l\rangle + C_{1,b}^{P_l}(t)|1, b, P_l\rangle + C_{0,a}^{P_l}(t)|0, a, P_l\rangle \right] \quad (3)$$

The summation over  $l$  signifies the accumulative nature of atomic quantized transverse momentum acquired during the atom-field interaction [64–67]. Furthermore,  $C_{j,k}^{P_l}$  represent probability amplitudes for  $k = a, b$  and  $j = 0, 1$  i.e. for  $j^{\text{th}}$  state of the cavity field and  $k^{\text{th}}$  atomic state. The larger value of atom-field detuning considered here is to ensure virtual Rabi cycles leaving negligible chance for spontaneously emitted photons, resulting in the guaranteed persistence of coherence throughout the interaction. Now solving the Schrodinger's wave equation i.e.  $i\hbar\frac{\partial}{\partial t}|\Psi_{AB}(t)\rangle = H|\Psi_{AB}(t)\rangle$ , using adiabatic approximation i.e.  $\Delta \gg \omega_r \gg \mu^2/\Delta$  yields the state vector as;

$$|\Psi(t)\rangle = \frac{1}{\sqrt{2}}[|0, b, P_o\rangle + |1, b, P_{-2}\rangle] \quad (4)$$

Here  $|P_o\rangle$  and  $|P_{-2}\rangle$  are the two mutually orthogonal split atomic momenta wavepackets yielded by off-resonant first order ABD when the interaction time is taken as,  $t = 2\pi\Delta/\mu^2$  [64–72]. For further mathematical details on quantum state engineering through ABD, one is referred to these well cited resources [17–19, 32, 70, 72]. The above equation shows that the atom is now entangled in only one degree of freedom i.e. atomic external quantized momentum  $|P_o\rangle(|P_{-2}\rangle)$  with the cavity-field. However, two spatially well separated split atomic wavepackets with ground states atomic signatures are travelling in mutually perpendicular directions rendered permissible under first order Bragg's diffraction after leaving the cavity. Thus we can expose any one momenta component to a laser beam for a pre-calculated time selected while keeping in view the classical longitudinal momentum or velocity of the atom. Under this semiclassical interaction scenario, the atom will be excited from the ground state  $|b\rangle$  to the excited state  $|a\rangle$  after interacting with the

laser field. Such an atom-field interaction is governed by the semiclassical interaction picture Hamiltonian as [73];

$$H^{sc} = \frac{\hbar\Omega_R}{2}[\sigma_{ab} + \sigma_{ba}] \quad (5)$$

Where,  $\Omega_R = |\wp_{ba}| \varepsilon / \hbar$  is Rabi frequency with  $\varepsilon$  describing the amplitude of applied classical field and  $\wp_{ba}$  represents the transition dipole matrix element. Moreover,  $\sigma_{ab}(\sigma_{ba})$  stands for atomic raising (lowering) operator operating under the due action of the classically applied field. Now solving the Schrodinger's wave equation and adjusting the interaction time to  $t_{sc} = \pi/\Omega_R$ , the final state vector comes to be;

$$|\Psi(t_{sc})\rangle = \frac{1}{\sqrt{2}}[|0, b, P_o\rangle - i|1, a, P_{-2}\rangle] \quad (6)$$

It is evident that Ramsey laser field was applied only to  $|P_{-2}\rangle$  component of the split atomic momenta wavepacket along Y-axis, the axis across which atomic momentum is again treated. The above equation stands for a hyperentangled state of two-level type-1 atom coherently correlated with the cavity field. The same procedure can be extended to engineer the  $n$ -partite hyperentangled state. For this purpose we pass a stream of two-level identical type-1 atoms through the cavity one by one under off-resonant ABD. This will consequently generate a state of the form expressed in eq. (4) but now with an entangled and extended Hilbert space. Then one of their spatially well separated momenta components interact with the classical laser fields under similar conditions as employed for the first atom. Therefore, the  $n$ -partite hyperentangled state becomes;

$$|\Psi\rangle = \frac{1}{2^{n/2}} \prod_{j=1}^n [|0, b^j, P_o^j\rangle + (i)^{3j} |1, a^j, P_{-2}^j\rangle] \quad (7)$$

Here the superscript  $j$  varies from 1 to  $n$  and stands for the number of identical atoms interacting with the cavity field consecutively, one after the other. This number  $n$  can be quite large in the range of thousands. This is because the experimental feasibility of such a large number of consecutive interactions has already been demonstrated within the permissible time limits of the onset of any appreciable decoherence [74, 75].

### III. Hyperentangled graph states engineering

#### A. Generation of hyperentangled cluster states

Expression (7) above, for any arbitrarily large  $n$ , represents a multipartite GHZ type hyperentangled atomic state tagged or coherently correlated with the cavity field because all these atoms have interacted successively with same cavity under off-resonant ABD. Now, it is evident that in order to engineer a pure hyperentangled atomic state, we have to disentangle the cavity field from this expression. More explicitly stated, we have to erase the cavity information appropriately to yield the intended multipartite hyperentangled atomic state. Thus in order to erase the cavity quantum information, we pass the auxiliary atom i.e. type-2 atom through the cavity resonantly for the removal of such quantum information. Since these auxiliary atoms are used to swap and subsequently erase the cavity-field information interactively for which one needs to invoke only the energy levels and therefore auxiliary atoms are taken to be moving with classical momentum. Moreover, the resonant atom should be considered initially in its ground state  $|g\rangle$  while its excited state is denoted by  $|e\rangle$ . Thus the initial state vector for such resonant interaction can be expressed as;

$$|\Psi(0)\rangle = \frac{1}{2^{n/2}} \prod_{j=1}^n [|0, b^j, P_o^j\rangle + (i)^{3j} |1, a^j, P_{-2}^j\rangle] \otimes |g\rangle \quad (8)$$

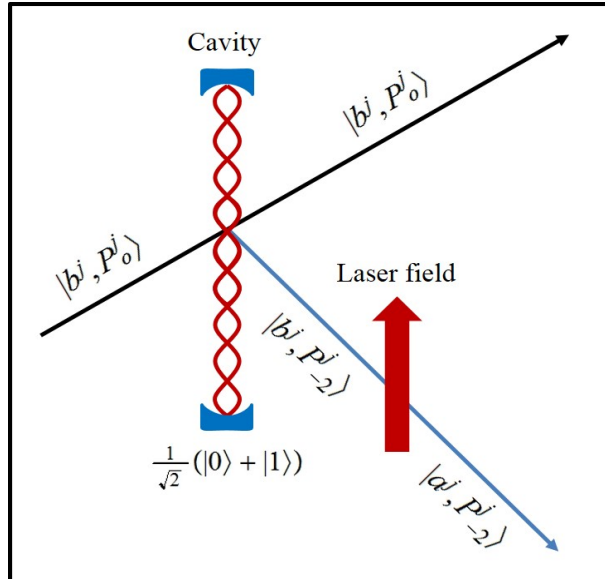


FIG. 1. Tagging of type-1 atoms with the cavity.

Here the tensor product incorporates the two set of atoms i.e. in the first product  $n$  atoms of type-1 that are appropriately entangled in momentum and internal degrees with the cavity field, whereas the outer product of type-2 atom that is needed to accomplish resonant interaction with the cavity field. As already stated, this interaction will swap the cavity information onto the initially ground state i.e.  $|g\rangle$  atom which will be subsequently erased via Ramsey field interactions. The interaction causing the cavity quantum information swapping is governed by the resonant atom-field interaction Hamiltonian given as under [73];

$$H = \hbar\mu[\sigma_{eg}\hat{c} + \hat{c}^\dagger\sigma_{ge}] \quad (9)$$

Here  $\sigma_{eg} = |e\rangle\langle g|$  ( $\sigma_{ge} = |g\rangle\langle e|$ ) denotes the atomic raising (lowering) operators and  $\mu$  is the atom-field coupling constant. This resonant atom-field interaction will result into the disentanglement of the cavity field from the entangled atoms. At this stage, the auxiliary atom will be energy-level wise entangled with the type-2 quantized momenta atoms. Hence auxiliary atom swaps the cavity information into its internal levels and leaves the cavity into vacuum state i.e.  $|0\rangle$  which can be traced out of the expression. This auxiliary atom is then employed for joining various building block states to engineer the desired graph state through resonant and dispersive interactions. Hence, in this way we can generate various type of cluster states and most general graph states of any arbitrary dimension with morphology encapsulating many nodes and edges. Prior to furnishing few easy but important examples in details to illustrate the case, it is worth clarifying here that the state expressed in eq. (8) should be taken as generic in the context of dimensionality and we can truncate it to express a hyper-superposition, with cavity information duly erased, of just a single atom to any higher dimensional hyperentangled atomic state, when and where required.

### B. Bipartite hyperentangled linear cluster states

For bipartite system we consider two type-1 atoms which are already tagged with their respective cavities i.e. cavity-1 and cavity-2 and two type-2 auxiliary atoms. Such an initial state may be expressed as follows;

$$|\Phi^1(0)\rangle = \frac{1}{\sqrt{2}}[|0_1, b^1, P_o^1\rangle - i|1_1, a^1, P_{-2}^1\rangle] \otimes |g_1\rangle$$

and

$$|\Phi^2(0)\rangle = \frac{1}{\sqrt{2}}[|0_2, b^2, P_o^2\rangle - i|1_2, a^2, P_{-2}^2\rangle] \otimes |g_2\rangle \quad (10)$$

The tensor product state therefore comes to be;

$$\begin{aligned}
|\Psi(t_1 = 0)\rangle &= |\Phi^1(0)\rangle \otimes |\Phi^2(0)\rangle \\
&= \frac{1}{2} [ |0_1, 0_2, b^1, b^2, P_o^1, P_o^2\rangle - i |0_1, 1_2, b^1, a^2, P_o^1, P_{-2}^2\rangle \\
&\quad - i |1_1, 0_2, a^1, b^2, P_{-2}^1, P_o^2\rangle - |1_1, 1_2, a^1, a_2, P_{-2}^1, P_{-2}^2\rangle ] \otimes |g_1, g_2\rangle
\end{aligned} \tag{11}$$

Now we pass 1<sup>st</sup> type-2 atom in its ground state  $|g_1\rangle$ , resonantly through cavity-1 and then dispersively through the cavity-2. Quantum information of the cavity-1 is thus swapped to this auxiliary atom and it leaves the cavity in vacuum state  $|0_1\rangle$ . This resonant interaction is governed by the Hamiltonian [eq. (9)] mentioned earlier. Then the same auxiliary atom, after swapping cavity-1 information via resonant interaction, enters into the cavity-2. Here in cavity-2, the auxiliary atom engages itself in dispersive interaction described by the Hamiltonian expressed in the coming paragraph. This dispersive interaction impart a field-dependent phase to the state in accordance with specifically selected interaction time. After that, we pass the second type-2 atom which is again initially prepared in its ground state  $|g_2\rangle$  from the cavity-2 resonantly that swaps the cavity information and leaves the cavity-2 in vacuum field state while transferring the cavity state information to the atom as was the case of first auxiliary atom. The resonant interaction time for both auxiliary atoms will be  $\pi$ -Rabi cycle i.e.  $t_1 = \pi/2\mu$ . Finally, to obtain the hyperentangled bipartite linear cluster state of type-1 atoms, we pass both the auxiliary atoms through the Ramsey field prior to the state-selective atomic detection immediately after leaving these cavities. Ramsey interactions are a stringent pre-requisite here because they erase the information carried by the auxiliary atoms. This is because the Ramsey's interaction leads to the transformations [73];

$$\begin{aligned}
|g_j\rangle &\longrightarrow \frac{1}{\sqrt{2}} [|g_j\rangle + |e_j\rangle] \\
|e_j\rangle &\longrightarrow \frac{1}{\sqrt{2}} [|g_j\rangle - |e_j\rangle]
\end{aligned} \tag{12}$$

The sequential interaction of these auxiliary atoms with the fields of the cavity is shown in the Fig. 2. Here we give a detailed step-wise description. The 1<sup>st</sup> auxiliary atom resonantly interacts with the cavity-1. Such a resonant atom-field interaction will swap the cavity-1's information. Thus the cavity is left in vacuum field state i.e.  $|0_1\rangle$  that can be simply traced out from the final equation. This atom-field resonant interaction is governed by the Hamiltonian i.e. eq. (9). Hence, setting an interaction time  $t_1 = \pi/2\mu$ , the initial state vector i.e. eq. (11) becomes;

$$\begin{aligned}
|\Psi(t_1)\rangle &= \frac{1}{2} [ |b^1, g^1, P_o^1\rangle - |a^1, e^1, P_{-2}^1\rangle ] \\
&\quad \otimes [ |0_2, b^2, P_o^2\rangle - i |1_2, a_2, P_{-2}^2\rangle ] \otimes |g^2\rangle
\end{aligned} \tag{13}$$

Now in the next step, the auxiliary atom-1, emerging from cavity-1 then dispersively interacts with cavity-2 and generates the desired entanglement by imparting local phase depending over amplitude of the cavity. This dispersive interaction is governed by the Hamiltonian [76];

$$H_d = \hbar\lambda \left[ \hat{c}\hat{c}^\dagger |e\rangle\langle e| - \hat{c}^\dagger\hat{c} |g\rangle\langle g| \right] \tag{14}$$

Where  $\lambda = \mu_d^2/\Delta$  is the effective Rabi frequency,  $\Delta$  is the detuning and  $\mu_d$  denotes the coupling parameter. This type of dispersive interaction has already been experimentally demonstrated in the context of quantum phase gate [77]. In our case it will assist to furnish the residual part of the Ising interaction joining the two

nodes. Therefore, the final state vector after dispersive interaction of auxiliary atom-1 with the cavity-2 for any arbitrary interaction time  $t_2$  becomes;

$$\begin{aligned}
|\Psi(t_2)\rangle = & \frac{1}{2} [ |0_2, b^1, b^2, g^1, P_o^1, P_o^2\rangle \\
& -i \exp(-i\lambda t_2) |1_2, b^1, a^2, g^1, P_o^1, P_{-2}^2\rangle \\
& + \exp(-2i\lambda t_2) |0_2, a^1, b^2, e^1, P_{-2}^1, P_o^2\rangle \\
& -i \exp(i\lambda t_2) |1_2, a^1, a^2, e^1, P_{-2}^1, P_{-2}^2\rangle ] \otimes |g^2\rangle
\end{aligned} \tag{15}$$

Now the auxiliary atom-2 which is initially prepared in its ground state  $|g^2\rangle$  resonantly interacts with cavity-2 for an interaction time  $t_3 = \pi/2\mu_r$  in order to swap the cavity information as already mentioned above. Such an interaction is governed by the resonant interaction picture Hamiltonian given in eq. (9). Therefore, using the initial conditions suggested by eq. (15), the final state vector after this resonant interaction lasting for time  $t_3 = \pi/2\mu_r$  yields the following state vector;

$$\begin{aligned}
|\Psi(t_3)\rangle = & \frac{1}{2} [ |b^1, b^2, g^1, g^2, P_o^1, P_o^2\rangle \\
& - \exp(-i\lambda t_2) |b^1, a^2, g^1, e^2, P_o^1, P_{-2}^2\rangle \\
& + \exp(-2i\lambda t_2) |a^1, b^2, e^1, g^2, P_{-2}^1, P_o^2\rangle \\
& - \exp(i\lambda t_2) |a^1, a^2, e^1, e^2, P_{-2}^1, P_{-2}^2\rangle ]
\end{aligned} \tag{16}$$

Thus in this way the cavity field information is effectively swapped through the auxiliary atom-2 and leaves the cavity-2 in vacuum field state  $|0_2\rangle$ , which is traced out from the above equation. Now, to engineer the desired hyperentangled state, we pass both these auxiliary atoms through the Ramsey zone after emerging out from the respective cavities prior to detection. This completes the eraser mechanism. Ramsey zone acts a symmetric Hadamard gate and will coherently split the atomic internal state in accordance with the transformations mentioned previously. Further, for the sake of symmetric, equally-weighted state engineering, the dispersive interaction time  $t_2$  carried previously as a running variable is now being fixed to  $t_2 = \pi/\lambda$ . Therefore, utilizing Ramsey transformations in eq. (16), the equal weighted atomic hyperentangled linear cluster states engineered in accordance with the state selective detection pattern of the auxiliary atoms come to be;

$$\begin{aligned}
|\Phi\rangle = & \frac{1}{2} \left[ \frac{1}{2} \{ |b^1, b^2, P_o^1, P_o^2\rangle + |b^1, a^2, P_o^1, P_{-2}^2\rangle \right. \\
& + |a^1, b^2, P_{-2}^1, P_o^2\rangle + |a^1, a^2, P_{-2}^1, P_{-2}^2\rangle \} \otimes |g^1, g^2\rangle \\
& \frac{1}{2} \{ |b^1, b^2, P_o^1, P_o^2\rangle - |b^1, a^2, P_o^1, P_{-2}^2\rangle \\
& + |a^1, b^2, P_{-2}^1, P_o^2\rangle - |a^1, a^2, P_{-2}^1, P_{-2}^2\rangle \} \otimes |g^1, e^2\rangle \\
& \frac{1}{2} \{ |b^1, b^2, P_o^1, P_o^2\rangle + |b^1, a^2, P_o^1, P_{-2}^2\rangle \\
& - |a^1, b^2, P_{-2}^1, P_o^2\rangle - |a^1, a^2, P_{-2}^1, P_{-2}^2\rangle \} \otimes |e^1, g^2\rangle \\
& \frac{1}{2} \{ |b^1, b^2, P_o^1, P_o^2\rangle - |b^1, a^2, P_o^1, P_{-2}^2\rangle \\
& - |a^1, b^2, P_{-2}^1, P_o^2\rangle + |a^1, a^2, P_{-2}^1, P_{-2}^2\rangle \} \otimes |e^1, e^2\rangle ]
\end{aligned} \tag{17}$$

It is evident from the above expression that for any atomic state detection permutation, we get a hyperentangled atomic linear cluster state. Further, from the procedure cited above, one can equally engineer any arbitrarily large  $n$ -partite atomic hyperentangled cluster state by coherently joining the states, taken initially from eq. (8) for large enough  $n$ , through the above explained Ising interaction.

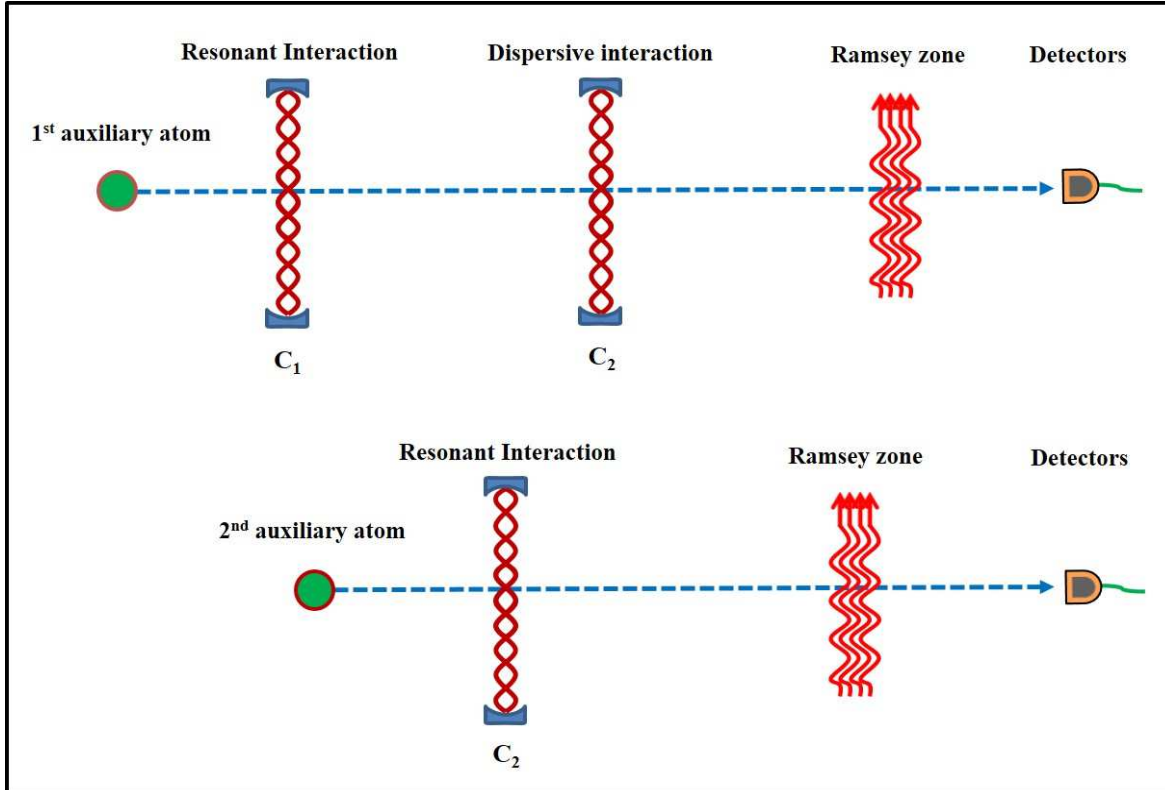


FIG. 2. The diagram represents the interaction of auxiliary atoms with the cavity-1 and cavity-2. Here  $|g\rangle$  and Here  $|e\rangle$  explore the ground and excited states of auxiliary atoms. Whereas,  $C_1$  and  $C_2$  stand for the cavity-1 and 2 respectively.

### C. Four-partite hyperentangled 2D-Cluster State

Following the previously explained procedure, here we give the schematics to generate the four-partite hyperentangled atomic 2D-cluster state. It is the most vital case because the counterpart photonic state was utilized for the experimental demonstration of one-way computing model [35]. Now, in order to engineer a four-partite hyperentangled atomic 2D-cluster state we consider four two-level type-1 atoms in which two of them say 1<sup>st</sup> and 2<sup>nd</sup> atom will pass through the cavity-1 and the remaining two atoms, say 3<sup>rd</sup> and 4<sup>th</sup> atom, will pass through the cavity-2 under off-resonant Bragg regime. These two-level neutral atoms are used to generate cavity-field entanglement as described earlier. In the next step, we assume two auxiliary atoms say type-2 atoms, which interact resonantly through their respective cavities to erase the cavities information in such a way that atom-1 after swapping information from cavity-1 through resonant interaction passes through cavity-2 where it interacts dispersively. Such dispersive interaction effectively form a controlled phase gate and thus entangle the two mutually independent states i.e. initially correlated state of atom-1, atom-2 and atom-3, atom-4. Therefore, the interaction ends up with the generation of the desired atomic hyperentangled state duly completed when these atoms traverse the Ramsey zone and are subsequently detected via state-selective detectors. These schematics are as illustrated in Fig. 3.

For the desired building block engineering as explained earlier, the 1<sup>st</sup> and 2<sup>nd</sup> type-1 atoms pass through the cavity-1 off-resonantly under atomic Bragg diffraction domain one after the other for an interaction time  $t = 2\pi\Delta/\mu^2$ . This coherently splits the atomic momenta wavepackets into two equal parts i.e. with equal probability amplitudes. After that one component of each atom is exposed to the classical laser field under the same conditions as proposed for eq. (6) to generate hyperentanglement. This procedure produces a pair



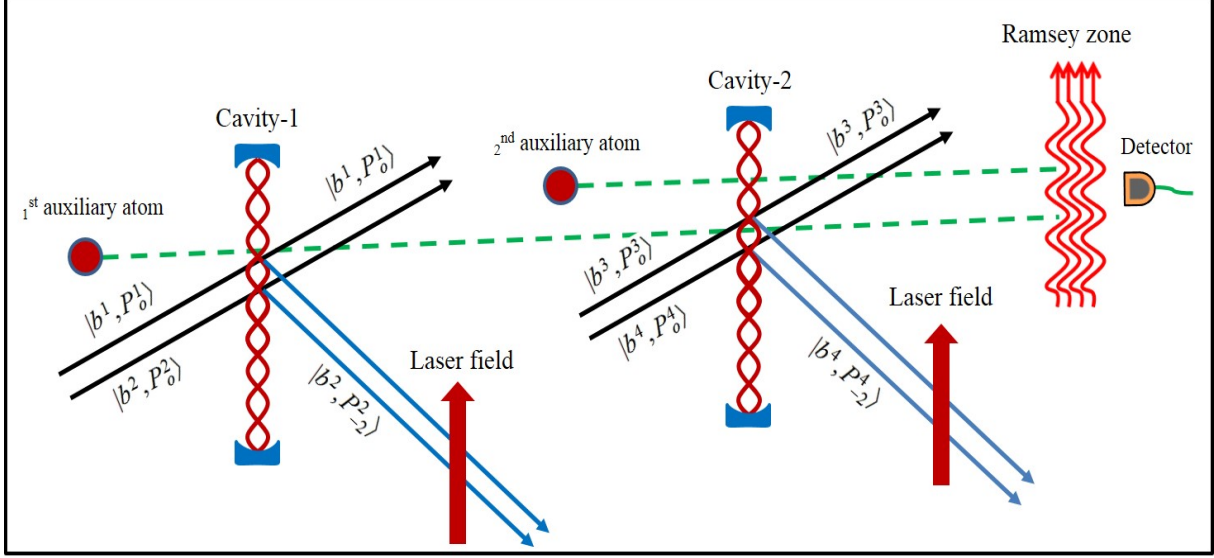


FIG. 3. The sketch elucidates the complete process of hyperentangled four-partite 2D-cluster state engineering. Here 1<sup>st</sup> and 2<sup>nd</sup> atom are off-resonantly Bragg diffracted from the cavity-1 and the interaction culminates into generating an entangled state of the form expressed in eq. (18) with the number fixed to  $n = 2$  in eq. (8). Whereas, the 3<sup>rd</sup> and 4<sup>th</sup> atom traverse off-resonantly through the cavity-2 in the same manner. Then the first auxiliary atom interacts resonantly with the cavity-1 and then dispersively with the cavity-2. Moreover, the 2<sup>nd</sup> auxiliary atom passes through the cavity-2 resonantly. Finally, these auxiliary atoms pass through the Ramsey zone for atomic state-selective detection.

of the GHZ type entangled states as follows;

$$|\Psi^{1,2}(t)\rangle = \frac{1}{\sqrt{2}} [|0_1, b^1, b^2, P_o^1, P_o^2\rangle + |1_1, a^1, a^2, P_{-2}^1, P_{-2}^2\rangle] \quad (18)$$

Similarly, the 3<sup>rd</sup> and 4<sup>th</sup> atom will pass through the cavity-2 off-resonantly repeating all the procedural steps as mentioned for 1<sup>st</sup> and 2<sup>nd</sup> atoms ends up with the generation of a similar doubly tagged or entangled state as follows;

$$|\Psi^{3,4}(t)\rangle = \frac{1}{\sqrt{2}} [|0_2, b^3, b^4, P_o^3, P_o^4\rangle + |1_2, a^3, a^4, P_{-2}^3, P_{-2}^4\rangle] \quad (19)$$

The next step is to erase the cavities information through the auxiliary atoms which will leave the cavities in their respective vacuum states and hence will disentangle the cavities which are left into respective vacuum state and hence can be traced out. Such auxiliary atoms are initially taken in their ground states  $|g^1\rangle$  and  $|g^2\rangle$  respectively, as depicted in the Fig. 3. Therefore, the initial product state, from eq. (18) and eq. (19) may be expressed as follows;

$$|\Psi^{2D}(0)\rangle = |\Psi^{1,2}(t)\rangle \otimes |\Psi^{3,4}(t)\rangle \otimes |g^1, g^2\rangle \quad (20)$$

Now the first auxiliary atom will interact resonantly for a complete  $\pi$ -Rabi cycle through the cavity-1 and then interacts dispersively with the the cavity-2 for an interaction time  $t_d$ . After that, the second auxiliary atom will pass through the cavity-2 resonantly, again for an interaction time equal to  $\pi$ -Rabi cycle. In this way, both the cavities's information gets completely swapped by these atoms. Thus both the cavities are left in their vacuum field states after such atom-field interactions. Therefore, the initial state vector i.e. eq.

(20) after such interactions transforms to;

$$\begin{aligned}
|\Psi^{2D}(t_d)\rangle = & \frac{1}{2} [|g^1, g^2, b^1, b^2, b^3, b^4, P_o^1, P_o^2, P_o^3, P_o^4\rangle \\
& + i \exp(-i\lambda t_d) |g^1, e^2, b^1, b^2, a^3, a^4, P_o^1, P_o^2, P_{-2}^3, P_{-2}^4\rangle \\
& + \exp(-2i\lambda t_d) |e^1, g^2, a^1, a^2, b^3, b^4, P_{-2}^1, P_{-2}^2, P_o^3, P_o^4\rangle \\
& - i \exp(i\lambda t_d) |e^1, e^2, a^1, a^2, a^3, a^4, P_{-2}^1, P_{-2}^2, P_{-2}^3, P_{-2}^4\rangle]
\end{aligned} \tag{21}$$

With the cavity fields  $|0_1\rangle$  and  $|0_2\rangle$  duly traced out of the above expression. Now, as stated in the previous section, these auxiliary atoms need to be disentangled from the above expression through Bell-basis measurement. For this purpose these auxiliary atoms are passed through the Ramsey zone immediately after emerging from the cavities. Such Ramsey zone enacts Hadamard transforms to the atomic internal states of the auxiliary atoms according eq. (12) prior to the state detection. Therefore, the final state vector carrying the state-selective detection pattern of the auxiliary atoms i.e.  $|g^1, g^2\rangle$ ,  $|g^1, e^2\rangle$ ,  $|e^1, g^2\rangle$  and  $|e^1, e^2\rangle$ , may be expressed as;

$$\begin{aligned}
|\Psi^{2D}\rangle = & \frac{1}{2} \left[ \frac{1}{2} \{ |b^1, b^2, b^3, b^4, P_o^1, P_o^2, P_o^3, P_o^4\rangle \right. \\
& + i \exp(-i\lambda t_d) |b^1, b^2, a^3, a^4, P_o^1, P_o^2, P_{-2}^3, P_{-2}^4\rangle \\
& + \exp(-2i\lambda t_d) |a^1, a^2, b^3, b^4, P_{-2}^1, P_{-2}^2, P_o^3, P_o^4\rangle \\
& \left. - i \exp(i\lambda t_d) |a^1, a^2, a^3, a^4, P_{-2}^1, P_{-2}^2, P_{-2}^3, P_{-2}^4\rangle \right\} \otimes |g^1, g^2\rangle \\
& + \frac{1}{2} \{ |b^1, b^2, b^3, b^4, P_o^1, P_o^2, P_o^3, P_o^4\rangle \\
& - i \exp(-i\lambda t_d) |b^1, b^2, a^3, a^4, P_o^1, P_o^2, P_{-2}^3, P_{-2}^4\rangle \\
& + \exp(-2i\lambda t_d) |a^1, a^2, b^3, b^4, P_{-2}^1, P_{-2}^2, P_o^3, P_o^4\rangle \\
& + i \exp(i\lambda t_d) |a^1, a^2, a^3, a^4, P_{-2}^1, P_{-2}^2, P_{-2}^3, P_{-2}^4\rangle \} \otimes |g^1, e^2\rangle \\
& + \frac{1}{2} \{ |b^1, b^2, b^3, b^4, P_o^1, P_o^2, P_o^3, P_o^4\rangle \\
& + i \exp(-i\lambda t_d) |b^1, b^2, a^3, a^4, P_o^1, P_o^2, P_{-2}^3, P_{-2}^4\rangle \\
& - \exp(-2i\lambda t_d) |a^1, a^2, b^3, b^4, P_{-2}^1, P_{-2}^2, P_o^3, P_o^4\rangle \\
& + i \exp(i\lambda t_d) |a^1, a^2, a^3, a^4, P_{-2}^1, P_{-2}^2, P_{-2}^3, P_{-2}^4\rangle \} \otimes |e^1, g^2\rangle \\
& + \frac{1}{2} \{ |b^1, b^2, b^3, b^4, P_o^1, P_o^2, P_o^3, P_o^4\rangle \\
& - i \exp(-i\lambda t_d) |b^1, b^2, a^3, a^4, P_o^1, P_o^2, P_{-2}^3, P_{-2}^4\rangle \\
& - \exp(-2i\lambda t_d) |a^1, a^2, b^3, b^4, P_{-2}^1, P_{-2}^2, P_o^3, P_o^4\rangle \\
& \left. - i \exp(i\lambda t_d) |a^1, a^2, a^3, a^4, P_{-2}^1, P_{-2}^2, P_{-2}^3, P_{-2}^4\rangle \right\} \otimes |e^1, e^2\rangle]
\end{aligned} \tag{22}$$

Hence, the above equation represents our desired four partite hyperentangled 2D-cluster states for example, if the detectors record  $|e^1, g^2\rangle$ , then the engineered equal-weighted four-partite hyperentangled 2D-cluster state can be expressed as;

$$\begin{aligned}
|\Psi^{e^1, g^2}\rangle = & \frac{1}{2} [|b^1, b^2, b^3, b^4, P_o^1, P_o^2, P_o^3, P_o^4\rangle \\
& + |b^1, b^2, a^3, a^4, P_o^1, P_o^2, P_{-2}^3, P_{-2}^4\rangle \\
& + |a^1, a^2, b^3, b^4, P_{-2}^1, P_{-2}^2, P_o^3, P_o^4\rangle \\
& - |a^1, a^2, a^3, a^4, P_{-2}^1, P_{-2}^2, P_{-2}^3, P_{-2}^4\rangle]
\end{aligned} \tag{23}$$

In expression (23), we have taken  $t_d = \pi/2\lambda$  instead of running variable for the sake of symmetry and simplicity. This is standard hyperentangled 2D-cluster atomic state whereas the rest of the equally probable states can be transformed into the desired standard form through local unitary operations or gates.

#### D. Hyperentangled Ring Graph State Engineering

Graph states represent the most generalized form for the multipartite entangled states including the commonly known states like Bell states, W-states and GHZ states. These specific cases can be engineered unitarily manipulating the relevant graph states through local operations. Graph states may incorporate a large number of qubits that can be binded into entangled correlations with diverse morphologies and geometries having multiple node connections among various graph edges. The ring graph state is a consecutively connected close ring of entangled qubits and generation of such states is vitally important for the construction of a quantum network that can be used for fast, secure and distributive quantum communication [78]. In this section, we propose a scheme to engineer a hyperentangled atomic ring graph state. It is based on  $n$ -number of type-1 two-level neutral atoms which interact off-resonantly with their respective cavities under Bragg regime and the interaction culminates into the generation of the entangled states of the type given in eq. (7). In the next step, an auxiliary two-level neutral atom i.e. type-2 atom, in its ground state  $|g\rangle$  will interact dispersively through the cavity-1 for an interaction time  $\pi$ -Rabi cycle. The same auxiliary atom is then passed through all of the other cavities, where it again interacts dispersively forming effectively a controlled phase gate through each atom-cavity field interaction and such interactions thus result in the generation of entanglements among the various cavities and their respective Bragg diffracted atoms. Now to connect the first and last cavity i.e. to produce the ring, we pass this same atom again through cavity-1 dispersively. After that such auxiliary atom is passed through the Ramsey zone for detection. This completes the procedure for the engineering of cavity field-Bragg diffracted atoms ring graph state. Finally we erase the quantum information carried by each cavity by passing  $n$ -auxiliary atoms, where one atom interacts resonantly with one specific cavity and swaps the field contained in the cavity. All these type-2 atoms, after passing through their specific cavities traverse Ramsey's zones and, are detected through state-selective detectors. This results into the generation of  $n$ -partite atomic ring graph state which can easily be transformed into a hyperentangled graph by exposing various sites with a classical laser beam for a pre-calculated time.

Below we present the mathematical details for the engineering of such a state in a self explanatory manner. We start from the entangled state i.e. eq. (4) engineered between the cavity-field and the off-resonantly Bragg diffracted atom from the cavity field. In the next step we pass an auxiliary atom which is initially prepared in its ground state  $|g\rangle$  through the cavity-1 dispersively. Thus the initial state vector for such an atom-field interaction may be engineered as follows;

$$\left| \Phi^1(t_1 = 0) \right\rangle = \frac{1}{\sqrt{2}} [ |0_1, b^1, P_o^1\rangle - i |1_1, a^1, P_{-2}^1\rangle ] \otimes |g\rangle \quad (24)$$

The Hamiltonian governing such a dispersive interaction is expressed in eq. (14). Thus, solution of the Schrodinger wave equation for an arbitrary interaction time  $t$  yields the state vector as;

$$\left| \Phi^1(t_1) \right\rangle = \frac{1}{\sqrt{2}} [ |0_1, g, b^1, P_o^1\rangle - i \exp(-i\lambda t_1) |1_1, g, a^1, P_{-2}^1\rangle ] \quad (25)$$

After successful completion of this process, the same auxiliary atom will pass through the second cavity, again in dispersive regime, to generate the entanglement between these cavities via controlled phase gate operation while taking  $t_1 = \pi/\lambda$ . Moreover, this atom-field interaction takes place under similar conditions as described in above equation without involving any external atomic momenta components because the auxiliary atoms are assumed to move with classical momentum. Thus the initial state vector for the second dispersive interaction i.e.  $\left| \Phi^2(t_2 = 0) \right\rangle = \frac{1}{2} [ ( |0_1, b^1, P_o^1\rangle + i |1_1, a^1, P_{-2}^1\rangle ) \otimes ( |0_2, b^2, P_o^2\rangle - i |1_2, a^2, P_{-2}^2\rangle ) ] \otimes$

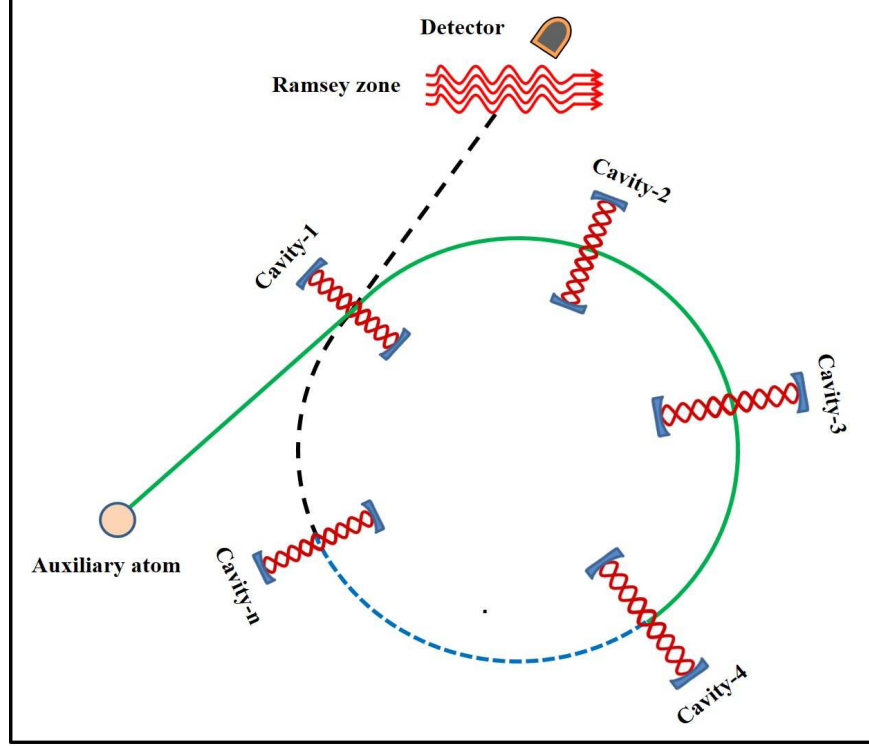


FIG. 4. The schematics explores the complete mechanism of atomic hyperentangled ring graph state engineering.

$|g\rangle$  transforms into the following state after dispersive interaction of the auxiliary atom with the second cavity:

$$\begin{aligned}
 |\Phi^2(t_2)\rangle &= \frac{1}{2} [ |0_1, 0_2, g, b^1, b^2, P_o^1, P_o^2\rangle \\
 &\quad + i \exp(-2i\lambda t_2) |0_1 1_2, g, b^1, a^2, P_o^1 P_{-2}^2\rangle \\
 &\quad - i \exp(-i\lambda t_2) |1_1, 0_2, g, a^1, b^2, P_{-2}^1, P_o^2\rangle \\
 &\quad + \exp(i\lambda t_2) |1_1, 1_2, g, a^1, a^2, P_{-2}^1, P_{-2}^2\rangle ]
 \end{aligned} \tag{26}$$

Similarly, passing the same auxiliary atom through  $n$ -number of cavities dispersively, one after the other, for an interaction time  $t = \pi/\lambda$  in each case, the final state vector can be expressed as;

$$|\Phi^n(t)\rangle = \left(\frac{1}{2}\right)^{\frac{n}{2}} \prod_{j=1}^n \left[ |0_j, b^j, P_o^j\rangle - \prod_{l=1}^{2n-1} (i)^{(2l+1)} |1_j, a^j, P_{-2}^j\rangle \right] \otimes |g\rangle \tag{27}$$

Now, in order to close the ring, we finally pass the auxiliary atom through cavity-1 again and invoke the same dispersive interaction. Therefore, the above generalized hyperentangled cluster state becomes;

$$|\Phi^{(n+1)}(t)\rangle = \left(\frac{1}{2}\right)^{\frac{n+1}{2}} \prod_{j=1}^{n+1} \left[ |0_j, b^j, P_o^j\rangle - \prod_{l=1}^{2n-1} (i)^{(2l+1)} |1_j, a^j, P_{-2}^j\rangle \right] \otimes |g\rangle \tag{28}$$

Furthermore, to swap the cavities information we pass  $n$ -extra auxiliary atoms resonantly through all of these cavities independently such that one resonant atom will interact only with one cavity. Such resonant atoms should be initially prepared in their ground states  $|g^{(i)}\rangle$ , where  $i = 1, 2, 3, \dots, n$ . These resonant individual

and independent atom-field interactions are governed by the interaction picture Hamiltonian given in eq. (9). Now these resonant atoms will swap the information of all cavities and left them in vacuum field states, respectively which can be traced out from the main expression. Finally, the resonant atoms carrying the quantum information will pass through the Ramsey zone and will be detected in their ground or excited states, respectively. Thus Bell-basis procedure is invoked to erase the cavity quantum information swapped and carried by these auxiliary atoms. Such state-selective detection of the  $n$ -auxiliary atoms finally yield us with  $2^n$  equally probable states corresponding to the detection sequence  $\prod_{j=1}^n \prod_{k=2}^n (\alpha^j, \beta^k)$  with  $(\alpha, \beta) = (e, g)$ .

Now if these all atoms are, for the sake of simplified presentation, assumed to be detected in their ground states then the corresponding engineered atomic hyperentangled ring graph state may be expressed as;

$$\left| \Phi^{(n+1)}(t) \right\rangle = \left( \frac{1}{2} \right)^{\frac{n+1}{2}} \prod_{j=1}^{n+1} \left[ |b^j, P_o^j\rangle + |a^j, P_{-2}^j\rangle \right] \quad (29)$$

Note that to engineer a hyperentangled ring graph state, the value of  $j$  must be greater than or equal to 2 i.e.  $j \geq 2$ . If  $j = 1$  then the state should only be a hyper-superposition state of a single atom. Thus for  $j = 2$ , the corresponding graph state should follow a triangular geometry. Similarly, for  $j = 3$ , it should be in the form of a square/rectangle. Therefore, any desired geometry hyperentangled graph state can be engineered through appropriate value of  $j$ .

### E. Dynamics of the Engineered states under Realistic Noise Environment

We have briefly described in the previous section as well as in the next section, the potentially stable nature of the engineered states qualitatively based on two very important features of such states.

1. Neutral ground state atoms interact off-resonantly with the field implying that there is almost nil chance for state decay and decoherence that results from spontaneous emission.
2. External quantized momenta states are known to be decoherence resistant states and are generally treated as the most fittest state under the domain of Quantum Darwinism [79].

After successful engineering of the different types of graph states, we are now in a position to characterize these states in term of the decay when they are coupled to a realistic classical environment. This mechanism will help us to assess the usefulness of these states for numerous quantum information tasks. It is evident that the actual potential of various quantum systems should be gauged in accordance with their respective preservation of the quantum coherence, entanglement and quantum information for longer time [80, 81]. Thus, a quantum system can be completely described when it is exposed to an environment. Therefore, we interact the currently engineered graph states with the classical fields for the purpose to evaluate the dynamical capacity of these graph states in the context of preservation of the entanglement for long enough times. Now keeping the importance of cluster states in view as well as for the sake of simplicity, we expose the cluster state i.e. eq. (17) to the Stochastic field expressed by the Hamiltonian [82];

$$\begin{aligned} H(t) = & H_1(t) \otimes I_2 \otimes I_3 \otimes I_4 + I_1 \otimes H_2(t) \otimes I_3 \otimes I_4 + \\ & I_1 \otimes I_2 \otimes H_3(t) \otimes I_4 + I_1 \otimes I_2 \otimes I_3 \otimes H_4(t). \end{aligned} \quad (30)$$

Here,  $H_n(t) = \xi I + \lambda \Delta_n(t) \sigma^x$  explores the Hamiltonian for a single qubit with  $n \in \{1, 2, 3, 4\}$  and  $I$  ( $\sigma^x$ ) is the identity matrix. Whereas, the  $\Delta_n(t)$  designates the Stochastic parameter which flips between  $\pm 1$ . Moreover,  $\lambda$  marks the coupling constant for the given quantum system and the environment. Now at any time  $t$ , the time evolved state for this system can be computed as  $\rho(t) = U(t)\rho(0)U^\dagger(t)$ . Where  $U(t) = \exp[-i \int_0^t H(t)dt]$  is the unitary time operator. Thus, in order to know about the nature of the system i.e. whether the system is separable or entangled, we find out the negative expectation values of the

time evolved matrix as  $EW(t) = \text{Tr}[R_O\rho(t)]$ , where  $R_O = \frac{1}{2}I - |W\rangle\langle W|$  is the witness operator [82, 83]. According to this criterion, the state will be separable for  $EW(t) \leq 0$  and will be entangled for  $EW(t) > 0$ .

Fig. 5 explores the dynamical capacity of the currently engineered graph state when coupled with the random field. It is clear from the graph that the state remains entangled for the whole interaction time. Thus, for  $\lambda = 0$  i.e. minimum interaction level, the state is maximally entangled but with the increase of the interaction between the system and environment, the state losses its entanglement very rapidly. Moreover, the sudden entanglement death and birth revivals are observed for any value of  $\lambda$  suggesting the transformation of the engineered graph state into a free or disentangled state as well as re-mergence of the entanglement. Thus, due to potential efficiency, the system quickly converts itself back into an entangled state [9, 84]. This inter-conversion of the graph state between the resource regime and free state occurs periodically as long as the system exposed to the classical field which concludes that the system effectively stays entangled for an infinite time. The plot also shows that the amplitude of entanglement does not vary with the time suggesting that the system regains its originality of the encoded entanglement. Therefore, from the above discussion, we can safely conclude that all of the currently engineered graph states are good resources for various quantum information protocols such as quantum networks and quantum computations. This claim, apart from the evaluated cluster state, is justified because all the state engineering is carried out via similar controlled phase gate operations

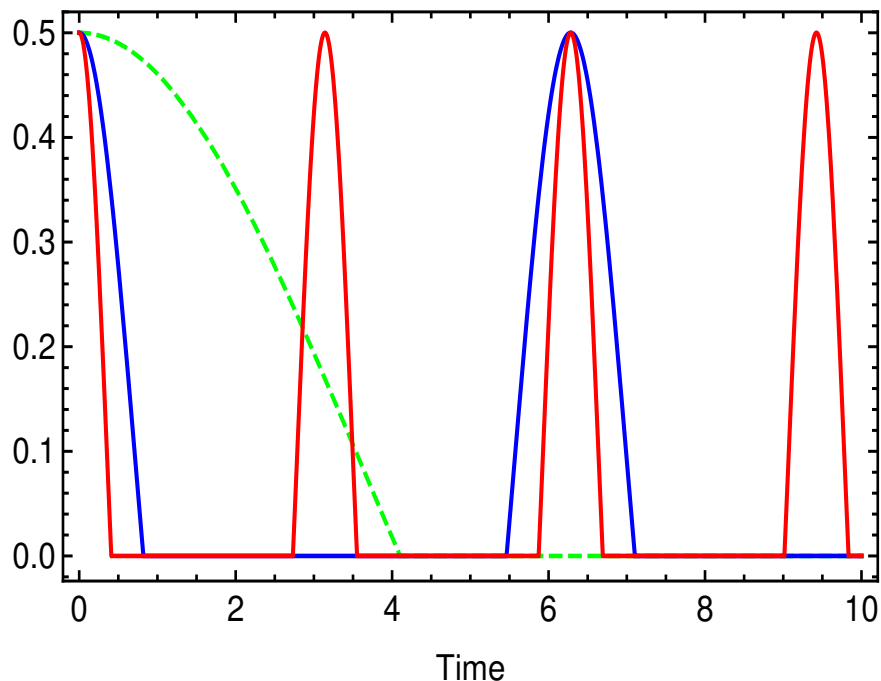


FIG. 5. The dynamical map of the engineered graph state coupled with the classical random field when  $\lambda = 0.1$  (green dashed line),  $\lambda = 0.5$  (Blue line),  $\lambda = 1$  (red line) with  $\Delta_1 = \Delta_2 = \Delta_3 = \Delta_4 = 1$  against the unitless time parameter  $t = 10$ .

#### IV. Experimental feasibility and Conclusion

The subject of Quantum information is now entering into more complex era comprised of multipartite quantum entangled webs with different graph morphologies [85, 86]. Recent explorations have amply demonstrated that quantum coherence prevailing among complex, multiqubit entangled system that generally fall into one type or the other of graph states can potentially explain many phenomena, and hitherto taken to be intractable [78, 87–90]. Therefore, such high dimensional, multipartite states and their indepth dynamical exploration is vitally important for the realization of quantum communication networks, distributed quan-

tum computing and the operational understanding of the biological phenomena [78, 91–97]. Cavity QED is a fundamental technique used to handle many quantum information tasks under ABD criteria [74, 75, 98, 99]. However, the experimental feasibility for the realization of such multipartite quantum networks is posed with a crucial problem i.e. the risk of decoherence. The main problem in generating these states can be subdivided into two major domains.

1. The engineering of hyperentangled atomic building block states i.e. state of the type expressed in eq. (6), mainly through off-resonant ABD.
2. The establishment of coherent connections among numerous graph edges and nodes with the help of Ising interactions carried mainly through dispersive atom-field interactions.

Now, for a long enough graph state a lot of atom-field interactions have to be sought out. So, as generally expected, the rate of decoherence should increase with the number of interactions seemingly making the present scenario apparently intractable experimentally. However, the situation is not that bleak in reality. This is because we use neutral atoms having quantized external momenta states that interact off-resonantly with the cavity field in our schematics. The advantage of these quantized momenta states of neutral atoms is that they minimize the threat of decoherence i.e almost nil chance of spontaneously emitted photons during these interactions. In fact these atomic quantized momenta states are recognized for their high resistance against decoherence and such states are considered to be the fittest states under what is known as Quantum Darwinism [79]. Moreover, the experimental feasibility of the interaction of large number of atoms i.e. in the range of thousands has already been demonstrated experimentally through high-Q cavities. Thus Quantum Darwinism guarantees the successful implementation and utilization of such states upto arbitrarily large number of atom-field interactions for longer enough times [100, 101]. Furthermore, the experimental demonstration of Bragg diffraction of atoms through classical as well as quantized fields have also been performed experimentally upto 8<sup>th</sup> order resulting in a significantly good spatial separations, efficiency and fringe visibility [29, 101–104]. Another state of the art experimental demonstration of the Bragg diffraction of <sup>85</sup>Rb atoms through a laser field of wavelength 780 nm has also been reported with good overall results [30]. Their employed working parameters nicely follows the criterion of the atomic Bragg diffraction and are summarized as follows;  $M = 85 \text{ amu}$  is the mass of the <sup>85</sup>Rb atom,  $\mu = 2\pi \times 16.4 \text{ MHz}$  is the vacuum Rabi frequency,  $\lambda = 780 \text{ nm}$  is the wavelength of the applied laser field and  $\omega_r = \hbar k^2/2M = 2.4 \times 10^4 \text{ rad/s}$  is the recoil frequency of the atoms. Moreover, the finesse of the cavity is  $F = 4.4 \times 10^5$  and the atom-field detuning is  $\Delta = 1 \text{ GHz}$ . As stated, these parameters are in good agreement with the off-resonant ABD criteria i.e  $\omega_r + \Delta \gg \mu\sqrt{n_c}/2$ . The most important aspect of in this context is the atom-field interaction time which is  $0.5\mu\text{s}$  and this is much smaller than the life-time of the cavity that is as high as fraction of a second [105–108]. On the other hand, one can also use helium atoms to experimentally demonstrate the atomic Bragg diffraction related state engineering with  $M = 4 \text{ amu}$ ,  $\omega_r = 1.06 \text{ MHz}$ ,  $\lambda = 543.5 \text{ nm}$ ,  $\Delta = 6.28 \text{ GHz}$ ,  $\mu^2/4\Delta = 120 \text{ kHz}$ ,  $F = 7.85 \times 10^6$  and  $t = 13 \mu\text{s}$  [64, 109]. Therefore, keeping the aforementioned experimental work in view, we are quite optimistic about the experimental execution of our work. Moreover, the proposed schematics are expected to yield good fidelities. It is important to note that the fidelities of cavity QED based atom-field interactions are hampered mainly by the interaction time errors encountered during such interactions. However, due to being long interaction time regime with spatially well separated outputs, ABD is generally not affected by such minor errors and using cold atom samples taken from Magneto-Optical Traps (MOT) further reduces such a stringent source of errors because cold atoms have almost no velocity spread [29, 102–104].

In summary, we have presented an experimentally executable scheme to engineer different type of hyperentangled cluster states along with the most general graph states which can be potentially employed for quantum communicational networks, distributed quantum computation as well as for understanding and simulating many complex phenomena including molecular dynamics, coherence effects in long, intricate

quantum multipartite chains and biological complexity prevailing in both zoological and botanical domains e.g. birds navigation and photosynthesis. It is worth noting here that Ising interaction comprised basically of dispersive and Ramsey interactions is generic in nature and can be easily employed to construct any envisionable graph morphology with arbitrarily large dimensionality. As already stated, such quantum states will play significant role in the future framework of quantum information along with the deeper knowledge of the working dynamics of various biological phenomena [110]. Moreover, as suggested by the invoked strategy and schematics, one can engineer any multipartite quantum network having diverse structural morphologies when and wherever needed for the study of any complicated, high dimensional quantum phenomenon. Similarly the exploration of these complex multipartite structures will enhance the operational knowledge of the holistic nature of quantum theory through multipartite coherence and interference effects [111]. In this work we have also shown that how one can hyper-superpose  $n$ -number of atoms connected with their respective cavities using off-resonant ABD. Here the cavities are considered as nodes i.e. the focal point from where we can inject, transfer and distribute the quantum information over an extended coherence pertaining zone. In addition, we have engineered a generalized  $n$ -nodes hyperentangled graph state by connecting cavities in the form of a ring. Such engineered state has its own figure of merits for quantum networks. Finally, we have discussed the experimental feasibility of our proposed scheme in light of the prevailing realistic laboratory parameters which guarantee the experimental demonstration of our proposed scheme.

#### Declarations

#### Acknowledgement

I. A. acknowledges Center for Computational Materials Science, University of Malakand, Pakistan for providing resources for conducting this research project. A. A. acknowledges Researchers Supporting Project, King Saud University, Riyadh, Saudi Arabia under grant number RSPD2024R666.

#### Ethical statement

All the results are original and analyzed analytically. The paper is neither submitted nor published in any other journal.

#### Declaration of competing interest

The authors declare that they have no known competing financial interests or personal relationships that could have appeared to influence the work reported in this paper.

#### Data availability statement

The data generated and/or analyzed during the current study are not publicly available for legal/ethical reasons but are available from the corresponding author on reasonable request.

---

## REFERENCES

- [1] A. Einstein, B. Podolsky, N. Rosen, "Can Quantum-Mechanical Description of Physical Reality Be Considered Complete?" *Phys. Rev.* **47**, 777-780 (1935).
- [2] R. P. Feynman, "Simulating physics with computers" *Int. j. Theor. phys.* **21**, 6/7 (2018).
- [3] A. Aspect, P. Grangier, G. Roger, "Experimental realization of Einstein-Podolsky-Rosen-Bohm Gedanken experiment: A new violation of Bell's inequalities" *Phys. Rev. Lett.* **49**(2), 91-94 (1982).
- [4] A. Aspect, J. Dalibard, G. Roger, "Experimental Test of Bell's Inequalities Using Time-Varying Analyzers" *Phys. Rev. Lett.* **49**(25), 1804-1807 (1982).
- [5] M. A. Nielsen, I. L. Chuang, "Quantum Computation and Quantum Information" Cambridge University Press, (London) (2002).
- [6] D. Bouwmeester, J. W. Pan, K. Mattle, M. Eibl, H. Weinfurter, A. Zeilinger "Experimental quantum teleportation" *Nature*, **390**(660), 575-579 (1997).



- [7] J. S. Bell, "On the Einstein podolsky rosen paradox" *Physics* **1**, 195-200 (1964).
- [8] M. Zidan, "A novel quantum computing model based on entanglement degree" *Mod. Phys. Lett. B* **34**, 2050401 (2020).
- [9] L. T. Kenfack, M. Tchoko, G. C. Fouokeng, L. C. Fai, "Dynamics of tripartite quantum correlations in mixed classical environments: the joint effects of the random telegraph and static noises" *Int. J. Quantum Inf.* **15**, 1750038 (2017).
- [10] J. M. Raimond, M. Brune, S. Haroche, "Manipulating quantum entanglement with atoms and photons in a cavity" *Rev. Mod. Phys.* **73** 565 (2001).
- [11] M. Brune, E. Hagley, J. Dreyer, X. Maitre, A. Maali, C. Wunderlich, J. M. Raimond, and S. Haroche, "Observing the Progressive Decoherence of the Meter in a Quantum Measurement" *Phys. Rev. Lett.* **77**(24), 4887-4890 (1996).
- [12] M. Zidan, A. Abdel, A. Younes, E. A. Zanaty, E. Khayat, M. Abdel, "A novel algorithm based on entanglement measurement for improving speed of quantum algorithms" *Appl. Math. Inf. Sci.* **12** 265 (2018).
- [13] H. Zhong et. al, "Quantum computational advantage using photons" *Science* **370**, 1460 (2020).
- [14] H. J. Kimble, "The quantum internet" *Nature* **453**, 1023, (2008).
- [15] P. G. Kwiat, "Hyper-entangled states" *J. Mod. Opt.* **44**, 2173 (1997).
- [16] T. Yang, Q. Zhang, J. Zhang, J. Yin, Z. Zhao, M. Zukowski, Z. B. Chen, J. W. Pan, "All-versus-nothing violation of local realism by two-photon, four-dimensional entanglement" *Phys. Rev. Lett.* **95**, 240406 (2005).
- [17] M. Nawaz, R. Islam, T. Abbas, M. Ikram, "Engineering quantum hyperentangled states in atomic systems" *J. Phys. B: At. Mol. Opt. Phys.* **50**, 215502 (2017).
- [18] M. Nawaz, R. Islam, T. Abbas, M. Ikram, "Remote state preparation through hyperentangled atomic states" *J. Phys. B: At. Mol. Opt. Phys.* **51**, 075501 (2018).
- [19] M. Nawaz, R. Islam, T. Abbas, M. Ikram, "Atomic Cheshire cat: untying energy levels from the de Broglie motion" *J. Phys. B: At. Mol. Opt. Phys.* **52**, 105501 (2018)
- [20] J. T. Barreiro, P. G. Kwiat, "Hyperentanglement for advanced quantum communication" *Proc. of SPIE* 7092 70920P (2008).
- [21] G. Y. Wang, Q. Liu, F. G. Deng, "Hyperentanglement purification for two-photon six-qubit quantum systems" *Phys. Rev. A* **94**, 032319 (2016).
- [22] X. L. Wang, X. D. Cai, Z. F. Su, M. C. Chen, D. Wu, L. Li, N. L. Liu, C. Y. Lu, J. W. Pan, "Quantum teleportation of multiple degrees of freedom of a single photon" *Nature* 518 516 (2015).
- [23] L. Ali, R. Islam, M. Ikram, T. Abbas and I. Ahmad, "Hyperentanglement teleportation through external momenta states" *J. P hys. B : A t. Mol . Opt. P hys.* **54** 235501(12pp) (2021).
- [24] L. Ali, R. Islam, M. Ikram, T. Abbas and I. Ahmad, "Teleportation of atomic external states on the internal degrees of freedom" *Quantum Inf. Process* **21**, 55(1-15) (2022).
- [25] L. Ali, R. Islam, M. Ikram, M. Imran and I. Ahmad, "Generation of maximally entangled N-photon field W-states via cavity QED" *Eur. Phys. J. Plus*, 137, 1236(1-12) (2022).
- [26] L. Ali, M. Ahmad, R. Islam, M. Imran, M. Ikram, I. Ahmad "Cavity-Assisted Atomic External Momenta State Teleportation" *Ann. Phys.* **536**(4), 2300277 (2024).
- [27] T. C. Wei, J. T. Barreiro and P. G. Kwiat, "Hyperentangled Bell-state analysis" *Phys. Rev. A* **75** 060305 (2007).
- [28] X. H. Li, S. Ghose, "Hyperentanglement concentration for time-bin and polarization hyperentangled photons" *Phys. Rev. A* **91** 062302 (2015).
- [29] S. Kunze, S. Durr, G. Rempe, "Bragg scattering of slow atoms from a standing light wave" *Europhys. Lett.* **34** 343 (1996).
- [30] S. Durr, T. Nonn, G. Rempe, "Origin of quantum-mechanical complementarity probed by a which-way experiment in an atom interferometer" *Nature* **395** 33 (1998).
- [31] R. Islam, T. Abbas and M. Ikram, "Biasing a coin after the toss: asymmetric delayed choice quantum eraser via Bragg regime cavity QED" *Laser Phys. Lett.* **12** 015203 (2015).
- [32] M. Ikram, M. Imran, T. Abbas and R. Islams, "Wheeler's delayed-choice experiment: A proposal for the Bragg-regime cavity-QED implementation" *Phys. Rev. A* **91** 043636 (2015).
- [33] R. Raussendorf, H. J. Briegel, "One-way quantum computation" *Phys. Rev.Lett.* **86**, 5188-5191 (2001).
- [34] M. A. Nielsen, "Cluster-state quantum computation" *Rep. Math. Phys.* **57**, 147-161 (2006).
- [35] P. Walther, K. J. Resch, T. Rudolph, E. Schenck, H. Weinfurter, V. Vedral, M. Aspelmeyer, A. Zeilinger, "Experimental one-way quantum computing" *Nature* **434**, 169-176 (2005).

- [36] S. M. A. Anis, T. Abbas, M. Imran and R. Islam, “Engineering quantum networks through Bragg diffracted hyperentangled atoms” *Phys. Scr.* **96** (2021) 125102.
- [37] D. E. Browne, T. Rudolph, “Resource-efficient linear optical quantum computation” *Phys. Rev. Lett.* **95**, 010501 (2005).
- [38] Y. Tokunaga, T. Yamamoto, M. Koashi, N. Imoto, “Simple experimental scheme of preparing a four-photon entangled state for the teleportation-based realization of a linear optical controlled-NOT gate” *Phys. Rev. A* **71**, 030301 (2005).
- [39] G. Vallone, E. Pomarico, F. De Martini, P. Mataloni, “One-way quantum computation with two-photon multi-qubit cluster states” *Phys. Rev. A* **78**, 042335 (2008).
- [40] Y. Tokunaga, S. Kuwashiro, T. Yamamoto, M. Koashi, N. Imoto, “Generation of high-fidelity four-photon cluster state and quantum-domain demonstration of one-way quantum computing” *Phys. Rev. Lett.* **100**, 210501 (2008).
- [41] W. B. Gao, X. C. Yao, P. Xu, H. Lu, O. Guhne, A. Cabello, C. Y. Lu, T. Yang, Z. B. Chen, J. W. Pan, “Bell inequality tests of four-photon six-qubit graph states” *Phys. Rev. A* **82**, 042334 (2010).
- [42] J. Cho, H. W. Lee, “Generation of atomic cluster states through the cavity input-output process” *Phys. Rev. Lett.* **95**, 160501 (2005).
- [43] P. Dong, Z. Y. Xue, M. Yang, Z. L. Cao, “Generation of cluster states” *Phys. Rev. A* **73**, 033818 (2006).
- [44] X. L. Zhang, K. L. Gao, M. Feng, “Efficient and high-fidelity generation of atomic cluster states with cavity QED and linear optics” *Phys. Rev. A* **75**, 034308 (2007).
- [45] J. Lee, J. Park, S. M. Lee, H. W. Lee, A. H. Khosa, “Scalable cavity-QED-based scheme of generating entanglement of atoms and of cavity fields” *Phys. Rev. A* **77**, 032327 (2008).
- [46] G. Li, S. Ke, Z. Ficek, “Generation of pure continuous-variable entangled cluster states of four separate atomic ensembles in a ring cavity” *Phys. Rev. A* **79**, 033827 (2009).
- [47] D. Gonta, T. Radtke, S. Fritzsche, “Generation of two-dimensional cluster states by using high-finesse bimodal cavities” *Phys. Rev. A* **79**, 062319 (2009).
- [48] D. Ballester, J. Cho, M. S. Kim, “Generation of graph-state streams” *Phys. Rev. A* **83**, 010302(R) (2011).
- [49] S. D. Barrett, P. Kok, “Efficient high-fidelity quantum computation using matter qubits and linear optics” *Phys. Rev. A* **71**, 060310(R) (2005).
- [50] L. M. Duan, R. Raussendorf, “Efficient quantum computation with probabilistic quantum gates” *Phys. Rev. Lett.* **95**, 080503 (2005).
- [51] Q. Chen, J. Cheng, K. L. Wang, J. Du, “Efficient construction of two-dimensional cluster states with probabilistic quantum gates” *Phys. Rev. A* **73**, 012303 (2006).
- [52] T. Tanamoto, Y. X. Liu, S. Fujita, X. Hu, F. Nori, “Producing cluster states in charge qubits and flux qubits” *Phys. Rev. Lett.* **97**, 230501 (2006).
- [53] Z. Y. Xue, G. Zhang, P. Dong, Y. M. Yi, Z. L. Cao, “Quantum controlled phase gate and cluster states generation via two superconducting quantum interference devices in a cavity” *Eur. Phys. J. B* **52**, 333-336 (2006).
- [54] X. L. Zhang, K. L. Gao, M. Feng, “Preparation of cluster states and W states with superconducting quantum-interference-device qubits in cavity QED” *Phys. Rev. A* **74**, 024303 (2006).
- [55] S. B. Zheng, “Generation of cluster states in ion-trap systems” *Phys. Rev. A* **73**, 065802 (2006).
- [56] P. J. Blythe, B. T. H. Varcoe, “A cavity-QED scheme for cluster-state quantum computing using crossed atomic beams” *New J. Phys.* **8**, 231 (2006).
- [57] N. Kiesel, C. Schmid, U. Weber, G. T. Th, O. G. H ne, R. Ursin, H. Weinfurter, Experimental analysis of a four-qubit photon cluster state. *Phys. Rev. Lett.* **95**, 210502 (2005).
- [58] N. Zhang, C. Y. Lu, X. Q. Zhou, Y. A. Chen, Z. Zhao, T. Yang, J. W. Pan, “Experimental construction of optical multiqubit cluster states from Bell states” *Phys. Rev. A* **73**, 022330 (2006).
- [59] Hein, J. Eisert, H. J. Briegel, “Multiparty entanglement in graph states” *Phys. Rev. A* **69**, 062311 (2004).
- [60] Islam, A. H. Khosa, H. W. Lee, F. Saif, “Generation of field cluster states through collective operation of cavity QED disentanglement eraser” *Eur. Phys. J. D* **48**, 271-277 (2008).
- [61] H. J. Briegel, R. Raussendorf, “Persistent entanglement in arrays of interacting particles” *Phys. Rev. Lett.* **86**, 910-913 (2001).
- [62] D. R. W. Briegel, “Stability of macroscopic entanglement under decoherence” *J. Phys. Rev. Lett.* **92**, 180403 (2004).
- [63] X. Zou, Y. Xiao, S. Li, Y. Yang and G. Guo, “Quantum phase gate through a dispersive atom-field interaction” *Phys. Rev. A*, **75**, 064301 (2007).

- [64] A. H. Khosa, M. Ikram, M. S. Zubairy, “Measurement of entangled states via atomic beam deflection in Bragg’s regime” *Phys. Rev. A* **70**, 052312 (2004).
- [65] A. H. Khosa, M. S. Zubairy, “Quantum-state measurement of two-mode entangled field-state in a high- Q cavity” *Phys. Rev. A* **72**, 42106 (2005).
- [66] A. H. Khosa, M. S. Zubairy, “Measurement of Wigner function via atomic beam deflection in the Raman-Nath regime” *J. Phys. B At. Mol. Opt. Phys.* **39**, 5079 –5 089 (2006).
- [67] A. A. Khan, M. S. Zubairy, “Quantum non-demolition measurement of Fock states via atomic scattering in Bragg regime” *Phys. Lett. A* **254**, 301 –3 06 (1999).
- [68] A. Khalique, F. Saif, “Engineering entanglement between external degrees of freedom of atoms via Bragg scattering” *Phys. Lett. A*, **314**, 37-43 (2003).
- [69] R. Islam, M. Ikram, F. Saif, “Engineering maximally entangled N-photon NOON field states using atom interferometer based on Bragg regime cavity QED” *J. Phys. B* **40**, 1359 1-368 (2007).
- [70] R. Islam, A. H. Khosa, F. Saif, “NOON and W states via atom interferometry” *J. Phys. B* **41**, 035505 (2008).
- [71] S. Qamar, S. Y. Zhu, M. S. Zubairy, “Teleportation of an atomic momentum state” *Phys. Rev. A* **67**, 042318 (2003).
- [72] R. Islam, M. Ikram, R. Ahmed, A. H. Khosa, F. Saif, “Atomic state teleportation, from internal to external degrees of freedom” *J. Mod. Opt.* **56**, 875 80 (2009).
- [73] M. O. Scully and M. S. Zubairy, *Quantum Optics* Cambridge University Press, Cambridge 1997.
- [74] S. Haroche, J. M. Raimond, “Exploring the Quantum: Atoms, Cavities and Photons” Oxford University Press, Oxford 2006.
- [75] S. Haroche, J.M. Raimond, “From cavity to circuit quantum electrodynamics” *Nat. Phys.* **16** 243-246 (2020).
- [76] M. S. Zubairy, G. S. Agarwal, M. O. Scully, “Quantum disentanglement eraser: a cavity QED implementation” *Phys. Rev. A* **70** 012316 (2004).
- [77] A. Rauschenbeutel, G. Nogues, S. Osnaghi, P. Bertet, M. Brune, J. M. Raimond, S. Haroche, “Coherent operation of a tunable quantum phase gate in cavity QED” *Phys. Rev. Lett.* **83**, 5166 –5 169 (1999).
- [78] I. Cohen and K. Molmer “Deterministic Quantum Network for Distributed Entanglement and Quantum Computation” *Phys. Rev. A*, **98**, 030302 (2018).
- [79] P. Ball, “Physics: Quantum all the way” *Nature* **453** 22 (2008).
- [80] A. U. Rahman, M. Noman, M. Javed, and A. Ullah, *Eur. Phys. J. Plus*, **136(8)**, 1-19 (2021).
- [81] A. U. Rahman, M. Noman, M. Javed, M. X. Luo, and A. Ullah, *Quantum Inf. Process.* **20(9)**, 1-20 (2021).
- [82] A. U. Rahman, M. Javed, and A. Ullah, Probing multipartite entanglement, coherence and quantum information preservation under classical Ornstein-Uhlenbeck noise. arXiv preprint arXiv:2107.11251.
- [83] A. U. Rahman, M. Javed, A. Ullah, and Z. X. Ji, *Quantum Inf. Process.* **20**, 321 (2021). <https://doi.org/10.1007/s11128-021-03257-z>.
- [84] L. Ali, A. U. Rahman, M. Imran, R. Islam, M. Ikram and I. Ahmad “The influence of mixed classical dephasing noisy channels on the dynamics of two-qubit correlations” *Opt. Quantum Electron.* **55**, 120 (2023).
- [85] C. Elliott “Building the quantum network” *New J. Phys.* **4**, 46 (2002).
- [86] C. Simon “Towards a global quantum network” *Nat. Photonics*, **11**, 678-680 (2017).
- [87] S. Lloyd “Quantum coherence in biological systems” *J. Phys. Conf. Ser.* **302**, 012037 (2011).
- [88] N. Lambert, Y. Chen, Y. Cheng, C. Li, G. Chen and F. Nori “Quantum biology” *Nat. Phys.* **9**, 10-18 (2013).
- [89] V. Gadiyaram, S. Vishveshwara and S. Vishveshwara “From Quantum Chemistry to Networks in Biology: A Graph Spectral Approach to Protein Structure Analyses” *J. Chem. Inf. Model.* **59(5)**, 1715-1727 (2019).
- [90] Y. Kim, F. Bertagna, E. M. Souza, D. J. Heyes, L. O. Johannissen, E. T. Nery, A. Pantelias, A. S. Jimenez, L. Slocombe, M. G. Spencer, J. Al-Khalili, G. S. Engel, S. Hay, S. M. Wilson, K. Jeevaratnam, A. R. Jones, D. R. Kattnig, R. Lewis, M. Sacchi, N. S. Scrutton, S. R. P. Silva and J. McFadden “Quantum Biology: An Update and Perspective” *Quant. Reports*, **3**, 1-48 (2021).
- [91] W. McCutcheon, A. Pappa, B. A. Bell, A. McMillan, A. Chailloux, T. Lawson, M. Mafu, D. Markham, E. Diamanti, I. Kerenidis, J. G. Rarity and M. S. Tame, “Experimental verification of multipartite entanglement in quantum networks” *Nat. Comm.* **7** 13251 (2016).
- [92] D. Cavalcanti, P. Skrzypczyk, G. H. Aguilar, R. V. Nery, P. H. Souto Ribeiro, S. P. Walborn, “Detection of entanglement in asymmetric quantum networks and multipartite quantum steering” *Nat. Comm.* **6** 7941 (2015).
- [93] S. Liao et.al, “Satellite-relayed intercontinental quantum network” *Phys. Rev. Lett.* **120**, 030501 (2018).
- [94] J. F. Dynes, A. Wonfor, W. W. S. Tam, A. W. Sharpe, R. Takahashi, M. Lucamarini, A. Plews, Z. L. Yuan, A. R. Dixon, J. Cho, Y. Tanizawa, J. P. Elbers, H. Greiber, I. H. White, R. V. Pentyl and A. J. Shields “Cambridge

- quantum network” *Nat. Photonics, J. Quant. Inf.* **5**, 101 (2019).
- [95] P. Ball “Physics of life: The dawn of quantum biology” *Nature*, **474**, 272-274 (2011).
- [96] M. Arndt, T. Juffmann and V. Vedral “Quantum physics meets biology” *HFSP J.* **3**, 386-400 (2009).
- [97] J. I. Cirac, A. K. Ekert, S. F. Huelga and C. Macchiavello “Distributed Quantum Computation over Noisy Channels” *Phys. Rev. A*, **59**, 4249 (1999).
- [98] R. G. Cortinas, M. Favier, B. Ravon, P. Mehaignerie, Y. Machu, J. M. Raimond, C. Sayrin, M. Brune, “Laser trapping of circular Rydberg atoms” *Phys. Rev. Lett.* **124** 123201 (2020).
- [99] P. Meystre, *Quantum optics: taming the quantum*. Springer, Switzerland (2021).
- [100] S. Deleglise, I. Dotsenko, C. Sayrin J. Bernu, M. Brune, J. M. Raimond, S. Haroche, “Reconstruction of non-classical cavity field states with snapshots of their decoherence” *Nature* **455** 510 (2008).
- [101] S. Gleyzes, S. Kuhr, C. Guerlin, J. Bernu, S. Deleglise, U. B. Hoff, S. Haroche, “Observing the quantum jumps of light: birth and death of a photon in a cavity” *Nature* **446** 297 (2007).
- [102] D. M. Giltner, R. W. McGowan, S. A. Lee, “Theoretical and experimental study of the Bragg scattering of atoms from a standing light wave” *Phys. Rev. A* **52** 3966 (1995).
- [103] P. J. Martin, P. L. Gould, B. G. Oldaker, A. H. Miklich D. E. Pritchard, “Diffraction of atoms moving through a standing light wave” *Phys. Rev. A* **36** 2495 (1987).
- [104] D. W. Vernooy, V. S. Ilchenko, H. Mabuchi, E. W. Streed H. J. Kimble, “High-Q measurements of fused-silica microspheres in the near infrared” *Opt. Lett.* **23** 247 (1998).
- [105] S. Durr, S. Kunze, G. Rempe, “Pendellosung oscillations in second-order Bragg scattering of atoms from a standing light wave” *Quantum Semiclassical Opt.* **8** 531-539 (1996).
- [106] P. Munstermann, T. Fischer, P. W. H. Pinkse, G. Rempe, “Single slow atoms from an atomic fountain observed in a high-finesse optical cavity” *Opt. Commun.* **159** 63-67 (1999).
- [107] P. Munstermann, T. Fischer, P. Maunz, P. W. H. Pinkse, G. Rempe, “Dynamics of single-atom motion observed in a high-finesse cavity” *Phys. Rev. Lett.* **82** 37913797 (1999).
- [108] T. Puppe, P. Maunz, T. Fischer, P. W. H. Pinkse, G. Rempe, “Single-atom trajectories in higher-order transverse modes of a high-finesse optical cavity” *Phys. Scr. T* **112** 7 (2004).
- [109] C. J. Hood, H. J. Kimble, J. Ye, “Characterization of high-finesse mirrors: Loss, phase shifts, and mode structure in an optical cavity” *Phys. Rev. A* **64** 033804 (2001).
- [110] M. Mohseni, Y. Omar, G. S. Engel, M. B. Plenio, “Quantum Effects in Biology” Cambridge University Press, Cambridge 2014.
- [111] Y. Aharonov, E. Cohen, J. Tollaksen, “Completely top-down hierarchical structure in quantum mechanics” *PNAS*, **115** 11730 (2018).